applied sciences

MDPI

Article

The Dynamic Cause of Volcanic Age Disparity in the Halmahera Arc, Eastern Indonesia, Based on Thermal Simulation

Gui Fang [1], Xuefeng Wang [1,*], Guozhang Fan [1], Hongping Wang [1], Guoping Zuo [1], Zhili Yang [1] and Jian Zhang [2]

[1] Petrochina Hangzhou Research Institute of Geology, Hangzhou 310023, China; fangg_hz@petrochina.com.cn (G.F.); fangz_hz@petrochina.com.cn (G.F.); wanghp_hz@petrochina.com.cn (H.W.); zuogp_hz@petrochina.com.cn (G.Z.); yangzl_hz@petrochina.com.cn (Z.Y.)

[2] College of Earth and Planetary Sciences, University of Chinese Academy of Sciences, Beijing 100049, China; zhangjian@mails.ucas.edu.cn

* Correspondence: wangxuef_hz@petrochina.com.cn

Abstract: A notable feature of volcanic activity in the Halmahera arc since the Middle Miocene is that eruptions have occurred episodically from south to north, rather than simultaneously. However, the dynamic cause of the volcanic age disparity between the northern and southern regions remains unresolved. To investigate this, thermal simulation methods were employed to calculate the temperature structures of the subducted slab and mantle wedge under varying movement rates of subduction and overriding plates. Simulation results indicate that arc magmatism is favored at lower subduction rates or higher overriding plate movement rates. During the Middle Miocene, the northward drift of the Australian plate propelled the Obi microplate southward via left-lateral strike-slip faults, accelerating its movement rate. In contrast, the movement rate of the Halmahera microplate in the north remained lower, unaffected by the Australian plate. The accelerated movement of the Obi microplate resulted in the rapid generation of a higher temperature zone, facilitating arc volcanism on Obi Island in the late Middle Miocene. Meanwhile, the lower movement rate of the Halmahera microplate delayed the formation of a favorable high-temperature zone for arc volcanism, leading to the emergence of volcanism on Halmahera Island in the late Pliocene.

Keywords: Halmahera volcanic arc; volcanic age disparity mechanism; subduction rate; overriding plate movement rate; thermal modeling

check for updates

Citation: Fang, G.; Wang, X.; Fan, G.; Wang, H.; Zuo, G.; Yang, Z.; Zhang, J. The Dynamic Cause of Volcanic Age Disparity in the Halmahera Arc, Eastern Indonesia, Based on Thermal Simulation. *Appl. Sci.* **2024**, *14*, 9896. https://doi.org/10.3390/app14219896

Academic Editor: Roberto Scarpa

Received: 23 August 2024
Revised: 22 September 2024
Accepted: 25 October 2024
Published: 29 October 2024

Copyright: © 2024 by the authors. Licensee MDPI, Basel, Switzerland. This article is an open access article distributed under the terms and conditions of the Creative Commons Attribution (CC BY) license (https://creativecommons.org/licenses/by/4.0/).

1. Introduction

Located to the southwest of the Philippine Sea Plate in eastern Indonesia, the Halmahera arc plays a crucial role in the southern part of the Pacific Plate arc tectonic zone [1]. As the sole Neogene volcanic arc in the world presently undergoing arc–arc collision, it is distinguished by notable volcanic activity [2–6]. This region is widely recognized as the "most diverse and complex" area pertaining to the formation of volcanic arcs and associated magmatism across the world [7].

There are two notable features of the volcanic activity in the Halmahera arc [8]. In the east–west direction, the entire arc has undergone episodic cessation of volcanic activity since the Pliocene, marked by the formation of fractures at multiple instances in various locations. Despite these interruptions, magmatism resumed promptly at new volcanic sites [9,10]. In the south–north direction, the volcanic age distribution along the entire Halmahera arc shows significant disparities. Rather than erupting simultaneously, the volcanic chain exhibits episodic volcanic activity traits. The volcanic age disparity between Obi Island in the south and the "K-shape" Halmahera Island in the north has been observed to be significant [11]. While the intermittent and migratory patterns of volcanic activity in the east–west direction have been well elucidated [12–15], there remains a lack of comprehensive studies addressing the volcanic age disparity in the north and south parts of

the Halmahera arc. This knowledge gap hinders the understanding of causal mechanisms, as noted by predecessors [16], with speculation that the surrounding plate movement differences may play a role [9,10]. The dense tropical rainforest covering the Halmahera arc complicates continuous geological boundary tracking on the surface, limiting available surface geology information. Consequently, geological investigations struggle to validate such speculations. Therefore, further insights into the volcanic age disparity between the northern and southern parts of the Halmahera arc may necessitate numerical simulations to deepen understanding and provide more robust explanations.

In our research, a dynamic model was developed using constraints from seismic tomography data. The deep thermal characteristics of the arc volcanoes with the westward subduction and retreat in the Halmahera subduction zone were simulated through the finite element method under various kinematic conditions. This can help in understanding the causes of volcanic age disparity in the Halmahera arc.

2. Geologic Setting

The intermittent and migratory nature of volcanic activity of the Halmahera arc is intricately linked to the retreat of the Halmahera subduction zone [8]. According to the Molucca Sea Plate evolution model [9,11,12,17–19], the Molucca Sea Plate, an oceanic plate that separated from the Philippine Sea Plate approximately 15 Ma, has descended into the mantle as a result of double subduction, convergence, and arc–arc collisions on both sides. Eastward subduction beneath Halmahera initiated approximately 11 million years ago (Ma) followed by a westward retreat of the subduction zone at a rate of 1–10 cm/a. Around 2 Ma, volcanic arcs on the eastern and western peripheries of the Molucca Sea began to collide. Analysis of seismic data suggests that during the late Pliocene or Pleistocene, a period of reduced volcanic and subduction activity occurred [12]. Geological investigations on Halmahera Island identify a brief interruption in volcanic activity during the Pleistocene (Figure 1a).

The age distribution of the Neogene volcanic arc (Figure 1b) reveals significant details about the evolution of volcanic activity in the Halmahera region. According to Baker and Malaihollo [11], volcanic activity in the Halmahera arc commenced around 11.5 Ma on Obi Island. The volcanic activity experienced interruptions between 11 and 9.5 Ma, followed by a northward migration starting around 9 Ma. Comparing the oldest volcanic age on Obi Island (11.5 Ma) with that of the central region of Halmahera Island (7.7 Ma), the northward migration of volcanic activity occurred at an estimated rate of approximately 6.5 cm/a [13]. Obi Island did not witness volcanic activity before 8 Ma, whereas volcanic rocks in Halmahera Island range in age from 8 Ma to 2 Ma [11]. Around 2 Ma, volcanic activity associated with the Halmahera arc was interrupted once again, followed by a westward migration of the frontal volcanic arc, leading to the onset of Quaternary volcanic activity (Figure 1a).

Examining Halmahera subduction and volcanic activity involves the analysis of two key elements: the stratigraphic history and the crust–mantle structure of the arc. Hamilton [1] originally suggested that the western part was a magmatic arc, whereas the eastern part was defined by a melange zone. The western region of Halmahera Island features an active volcanic arc, with its basement mainly covered by Neogene sedimentary and pyroclastic rocks whose exact lithology and age are uncertain [13,19]. This suggests that the present volcanic basement in western Halmahera originated from the Late Oligocene to Early Miocene period, following the erosion of the Late Cretaceous to Early Tertiary volcanic arc [20]. Conversely, the eastern basement of Halmahera Island is composed of ophiolite formations mixed with Mesozoic and Eocene sedimentary rocks. Since the Middle Oligocene, this sequence has been overlain unconformably by sedimentary and volcanic deposits [21]. During the early Oligocene, the eastern basement of Halmahera underwent uplift and substantial erosion, followed by gradual subsidence in the middle to late Oligocene [1]. In the Miocene, subsidence progressed from east to west, with the Pliocene seeing an increase in volcanic activity in the eastern region affected by the western

volcanic arc [11]. By the Middle Pleistocene, intense deformation led to significant tilting of boundary blocks, extensive folding, and thrusting along both the eastern and western margins of Halmahera Island.

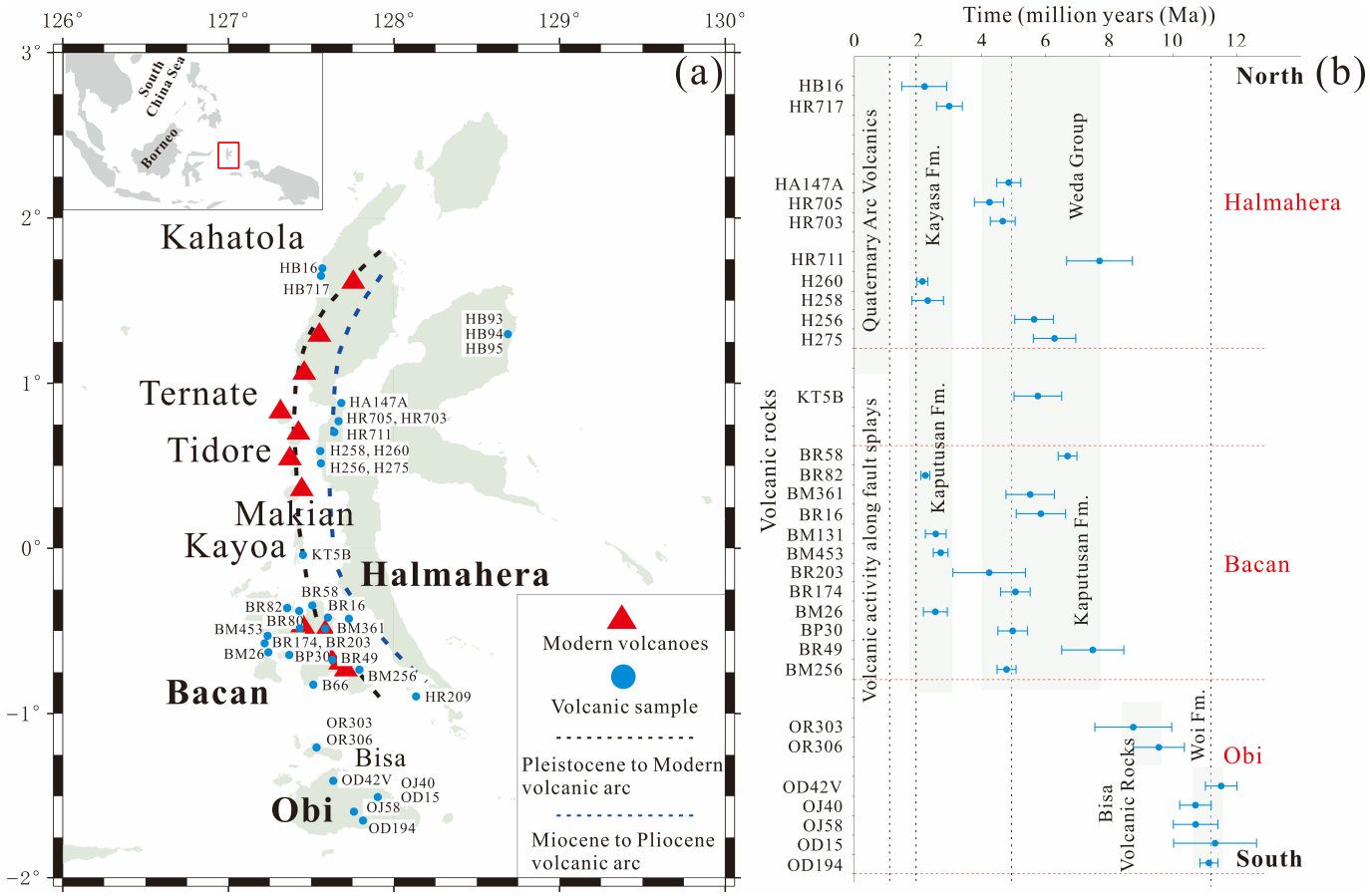


Figure 1. Distribution and dating results of volcanic rock samples in the Halmahera arc. (**a**) The distribution of arc volcanoes and rock samples in the Halmahera area (blue dots for sampling sites, red triangles for modern volcanoes, modified after [11]; the blue dashed line is the location of the Miocene–Pleistocene volcanic arc, and the black dashed line is the location of the Pleistocene–present volcanic arc, modified after [8]). (**b**) Dating of volcanic rock samples from the Halmahera arc, data are from [11].

The pre-Neogene geology of the Halmahera region consists of a basement of ophiolitic and arc-related rocks overlain by and imbricated with arc volcanic, plutonic, and sedimentary rocks of the late Mesozoic to Eocene age [11,15]. Following an Eocene unconformity (possibly linked with the Pacific plate reorganization at this time) a Late Eocene arc developed with associated basaltic pillow lavas and volcaniclastic turbidites; this arc ceased activity in the earliest Miocene and its termination is marked by a regional unconformity. Middle Miocene limestones were deposited throughout the region during a period of stability before the development of the Neogene arc and associated sedimentary rocks [17,21]. Deformation in the Pliocene is marked by another unconformity. Continental metamorphic rocks representing the Australian crust and possibly of Paleozoic or younger ages are juxtaposed against ophiolitic rocks in the southern part of the region [18].

Seismic, gravity, and magnetic data constitute the primary datasets for investigating the crust–mantle structure in this region. Currently, Halmahera Island is experiencing a dense distribution of seismic events. Figure 2a depicts the spatial distribution and magnitudes of seismic events recorded from 2000 to 2020 in this area. In the Molucca Strait, intermediate- and shallow-focus earthquakes (depicted as blue dots in Figure 2a)

are densely concentrated, while deep-focus earthquakes (represented by green and yellow dots in Figure 2a), which occur at depths greater than 100 km, are predominantly located in the western part of the Halmahera volcanic arc [20]. This distribution indicates a gradual deepening of the Benioff zone from the Molucca Strait to the Halmahera arc. Figure 2a$_1$ shows the profile of wave velocity anomaly *dVp* based on the global wave velocity model UU-P07. Beneath the Halmahera volcanic arc, an eastward-tilted high-velocity *dVp* anomaly is observed, adjacent to a relatively extensive low-velocity dVp anomaly to the east of this high-velocity zone. The high-velocity *dVp* anomaly corresponds to the Molucca Sea Plate, which is gradually subducting into the mantle with a depth of 250 km, while the low-velocity *dVp* anomaly represents the overriding lithospheric plate to the east [15].

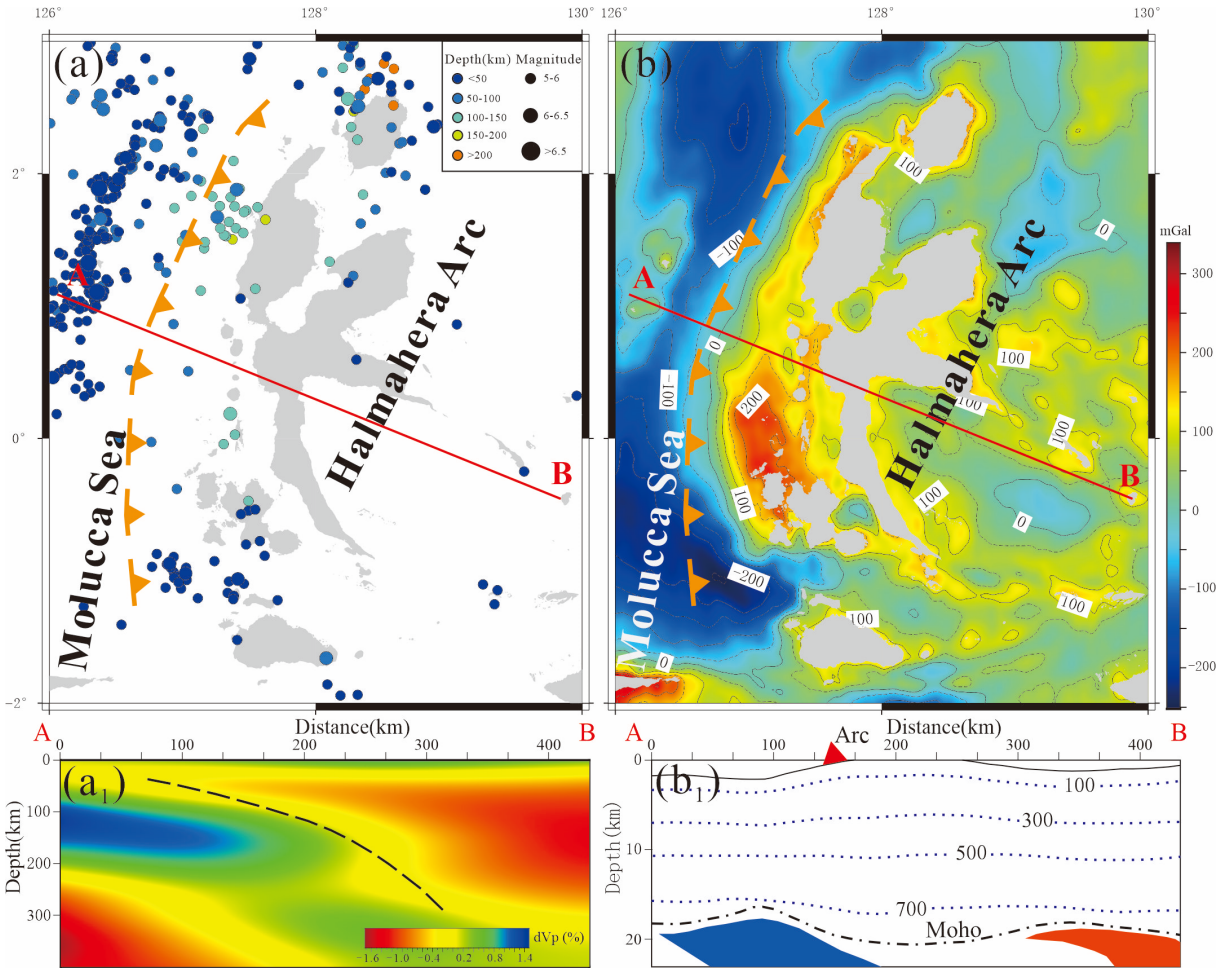


Figure 2. Geophysical characteristics of Halmahera arc. (**a**) Distribution of seismic events; data are from the International Seismological Centre [22], where (**a$_1$**) is wave velocity anomaly *dVp* of seismic *Vp* in A–B profile. Data are from global wave velocity anomaly model UU-P07 [23]. (**b**) Free-air gravity anomaly; data are from the global gravity database TOPEX [24], where (**b$_1$**) is temperature structure calculated by magnetic anomaly and Curie point, and the Moho depth inversion from the free-air gravity anomaly in A–B profile [25].

Figure 2b displays the free-air gravity anomaly across the Halmahera region, with a spatial resolution of one minute timing one minute ($1' \times 1'$). The gravity anomaly across Halmahera Island is notably elevated, with the peak value located westward of Halmahera Island aligning with the volcanic arc [26], whereas the Moluccan Sea exhibits a low gravity anomaly. Towards the eastern part of Halmahera Island, the gravity anomaly pattern corresponds to a northwestward structural trend, indicative of the shallow tectonic evolution during the westward retreat of the Halmahera subduction zone. The Moho

surface under the volcanic arc of Halmahera slopes to the east with a deep depth exceeding 20 km. The temperature of the Moho surface exceeds 700 °C, with an average geothermal gradient of approximately 3–4 °C/100 m (Figure 2b$_1$).

3. Model and Method

3.1. Numerical Model Design for Thermal Simulations

The relatively young oceanic plate material has been generally too buoyant to undergo significant subduction to great depths; instead, it can only be pushed horizontally beneath the overriding plate. For instance, beneath the Halmahera volcanic arc, located on the eastern flank of the Molucca Sea Plate, subduction has progressed to a depth of up to 450 km at an angle of approximately 45°, characterized by continuous retreat since 10 Ma [6]. Taking Mindanao Island as a kinematic reference point, the Halmahera subduction zone along the eastern margin of the Molucca Sea Plate is currently retreating westward at a rate of approximately 7 cm/year, while simultaneously subducting eastward at around 2 cm/year [4]. Nevertheless, the geological dynamics of subduction and convergence around the Molucca Sea Plate are irregular, characterized by varying rates of subduction and convergence on either side [27].

Assuming that the subduction rate is represented by V, which has horizontal (Vx) and vertical (Vz) components, along with a movement rate U for the overriding plate (see Figure 3a), several conditions can be examined. When $U - Vx = 0$, the position of the subduction zone remains stable, and both the arc and the trench retain fixedness. Conversely, when $U - Vx > 0$, the subduction zone retreats, urging the arc to migrate backward along with the trench (Figure 3a).

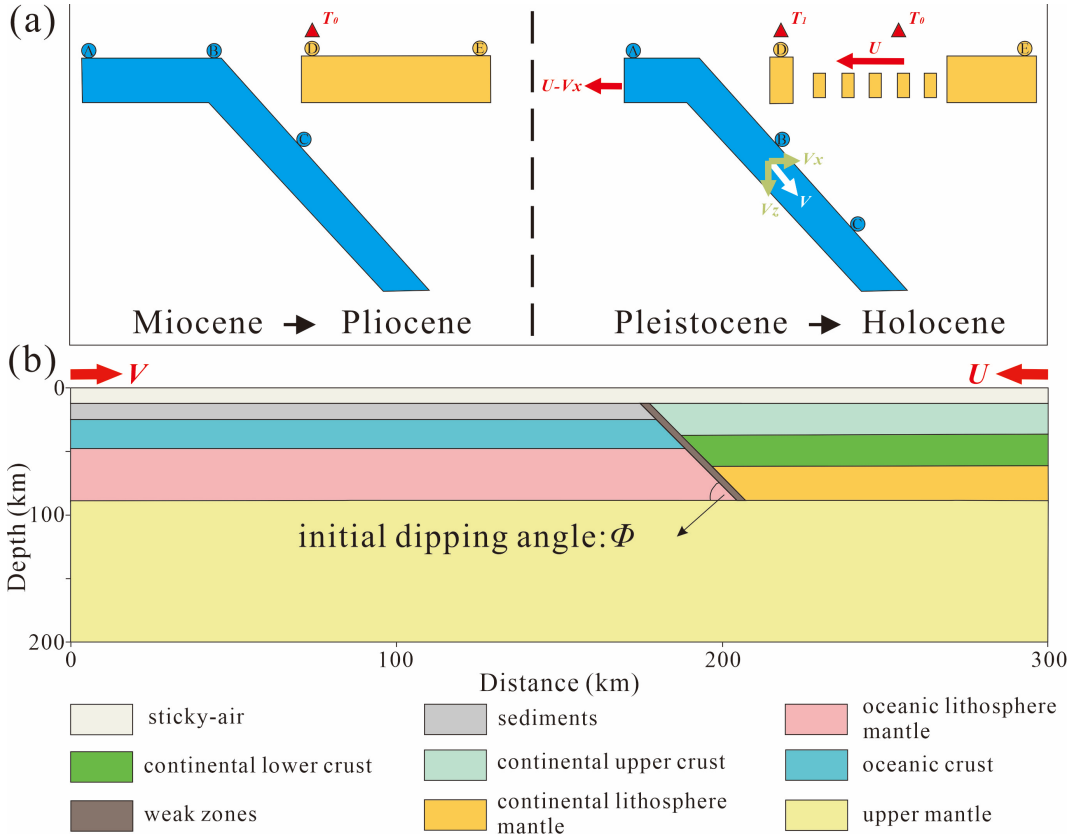


Figure 3. (**a**) The subduction retreat kinematics model of Halmahera volcanic arc; (**b**) two-dimensional initial geometric model of subduction zone, where V is the subduction rate, U is the overriding plate movement rate, and Φ is the initial subduction angle.

With reference to earlier subduction models conducted in this region [28–30], we set up four distinct subduction models, depicted schematically in Figure 3b. Each model spanned 300 km in length and extended to a depth of 200 km. The weak zone width was set at 5 km, while the sticky-air layer thickness was 10 km across all models. Here, V represents the subduction rate, U denotes the movement rate of the overriding plate, and Φ signifies the initial subduction angle. The varying geometric parameters for each specific model are presented in Table 1. The models were discretized with a minimum grid resolution of 2×2 km.

Table 1. Parameters of the geometric models.

Model Name	Initial Overriding Plate Length (km)	Initial Subducting Plate Length (km)	Initial Dipping Angle	Initial Subduction Rate V (mm/a)	Initial Overriding Plate Movement Rate U (mm/a)
Case 1	100	200	45°	30	60
Case 2	100	200	45°	30	40
Case 3	100	200	45°	20	50
Case 4	100	200	45°	40	50

It should be noted that the variation of the subduction angle was an important factor leading to the generation of the volcanism. However, due to the relatively younger subduction zone beneath the Halmahera arc, there is no historical record of the changes in subduction angle or the associated volcanic activity during transient subduction. As a result, the effect of variations in the subduction angle is not taken into account in our simulation models.

3.2. Applied Numerical Methods and Simulation Parameters

Deformation at the lithospheric scale can be modeled as a quasi-static thermomechanical coupling process. To simulate subduction, we solve the three conservation equations for momentum, mass, and heat [28]. The computations were performed using ASPECT version 2.2.0. The Stokes equation is expressed as follows:

$$-\nabla\cdot[2\eta(\varepsilon(\boldsymbol{u}))] + \nabla p = \rho g \tag{1}$$

In this equation, η represents the coefficient of viscosity, while $\varepsilon(\boldsymbol{u})$ denotes the strain rate, defined as $\varepsilon(\boldsymbol{u}) = \frac{1}{2}\left(\nabla\boldsymbol{u} + \nabla\boldsymbol{u}^T\right)$, where u is the velocity and p is the pressure. The acceleration of gravity, g, is 9.8 m/s^2. The density, ρ, is approximated using the Boussinesq assumption for small temperature variations: $\rho = \rho_0(1 - \alpha(T - T_0))$, where T_0 is the reference temperature, α is the thermal expansion coefficient, and ρ_0 is the reference density at temperature $T = T_0$. The equations for mass conservation (Equation (2)) and heat conservation (Equation (3)) are as follows:

$$\nabla\cdot\boldsymbol{u} = 0 \tag{2}$$

$$c\rho\frac{\partial T}{\partial t} + c\rho v\cdot\nabla T = K\nabla^2 T - \rho SL + Q \tag{3}$$

where c is the specific heat, ρ is the density, v is the velocity, T is the temperature, t is the time, K is the thermal conductivity, L is the latent heat of melting, S is the rate of melting, and Q is the radiogenic heat production rate. The parameters used in the simulations (Table 2) refer to previous research [29]. The depth-dependent mantle solidus and liquidus temperatures used in our calculations are discussed bellow.

Table 2. Physical and Geometrical Parameters of the model.

Parameters	Mantle	Sediments	Ocean Crust	Weak Zone	Upper Crust	Lower Crust
Space (km)	85	5	10	15	20	15
Thermal conductivity ($W \cdot m^{-1} \cdot K^{-1}$)	3.3	0.85	2.5	2.5	2.5	2.5
Specific heat capacity ($J \cdot kg^{-1} \cdot K^{-1}$)	750	750	750	750	750	750
Density ($kg \cdot m^{-3}$)	3100	2300	2900	2900	2700	2800
Thermal expansion (K^{-1})	2×10^{-5}	2×10^{-5}	2×10^{-5}	2×10^{-5}	2×10^{-5}	2×10^{-5}
Angles of internal friction (°)	20	5	10	2	20	20
Cohesions (Pa)	20×10^6	1×10^6	1×10^6	1×10^6	20×10^6	20×10^6
Grain size exponents	3	1	1	1	1	1

A computational model was established with two dimensions: 300 km in width and 200 km in depth. The model incorporated a range of kinematic velocities for the Halmahera volcanic arc, where ($U - Vx > 0$) indicated conditions favoring plate retreat. The boundary conditions for the models were established as follows: both the top and bottom sides were free to slide, while the left and right sides were designated as velocity boundaries. Different subduction rates V were applied in relation to the overriding plate movement rate U. The boundary temperature was determined using the half-space cooling model as outlined by [30–32]:

$$T = T_0 + (T_1 - T_0)\frac{Z}{dZ} \quad (4)$$

here Z is the thickness. A constant temperature of 5 °C is assumed to be maintained at the upper boundary, with the western boundary being adiabatic and the lower boundary set to 1350 °C.

4. Results

4.1. Case 1 and Case 2: Same Subduction Rates, Different Overriding Plate Movement Rates

Figure 4 depicts the thermal structure of the subduction zone located beneath the Halmahera volcanic arc. This model was created with a constant subduction rate V_0 (around 3 cm/a), but with different rates for the movement of the overriding plate U. Specifically, Case 1 involves an overriding plate movement rate U_1 of approximately 6 cm/a, whereas Case 2 has a rate U_2 of about 4 cm/a.

The results indicate that a high-temperature wedge zone developed beneath the Halmahera volcanic arc due to the westward movement of the plate. In Case 1, where the overriding plate movement rate significantly exceeded the subduction rate ($U_1 >> V_0$), a prominent high-temperature geosynclinal area emerged. Extended periods of rapid convergence could result in unusually high temperatures (Figure 4b_1) at depths ranging from 10 to 20 km, potentially reaching the melting point of hydrated mantle rock, which could affect arc magmatism.

On the other hand, in Case 2, where the rate of movement of the overriding plate was only slightly higher than the subduction rate ($U_2 > V_0$), the subduction zone beneath the Halmahera volcanic arc, characterized by lower temperatures, expanded. Over time, the temperature within the mantle wedge decreased (refer to Figure 5c_1), leading to a gradual decline in arc magmatism. Comparison of Case 1 and Case 2 suggests that when the subduction rate remains constant, a faster movement rate of the overriding plate promotes higher temperatures in the mantle wedge. This increase in temperature favors the partial melting of mantle material, leading to enhanced arc magmatic activity.

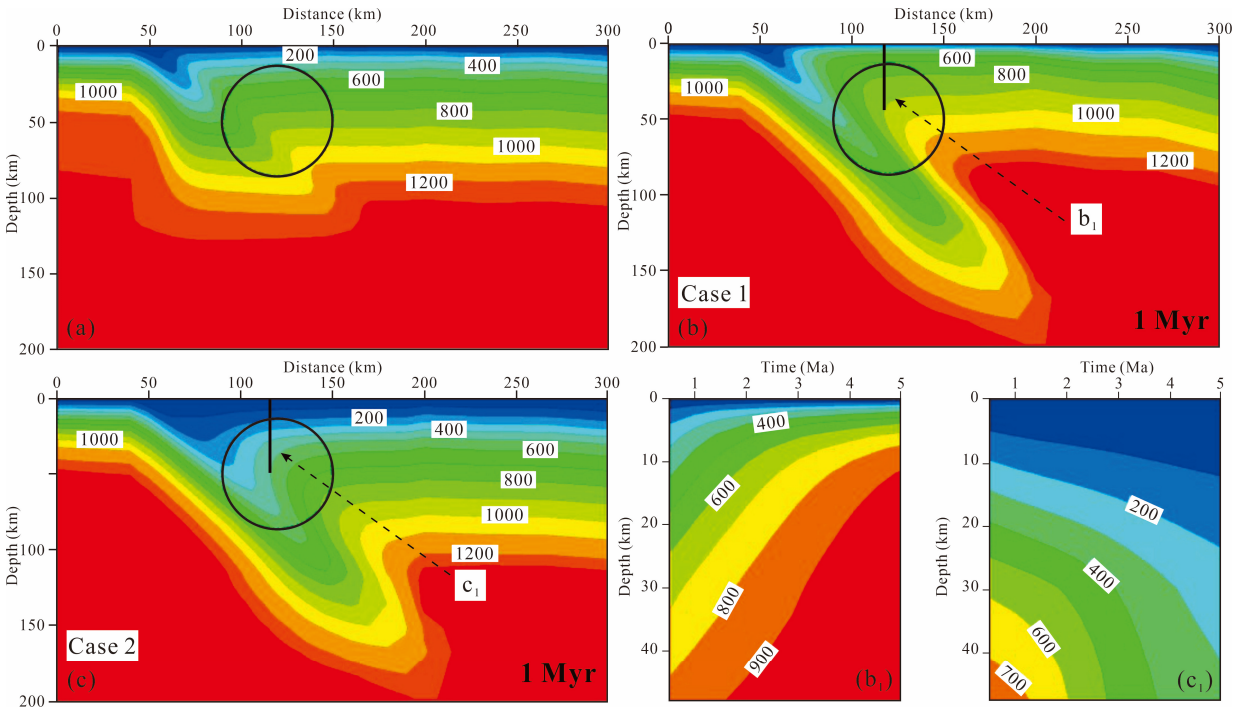


Figure 4. The effect of the overriding plate movement rate U on the evolution of thermal structure. (**a**) The current thermal structure, with units in °C; (**b**) Case 1: the thermal structure after 1 Myr at a higher overriding plate movement rate U_1, also in °C, where (**b$_1$**) shows the evolution of the thermal structure above the subducted slab over 0 to 5 Myr at the higher rate U_1; (**c**) Case 2: the thermal structure after 1 Myr at a lower overriding plate movement rate U_2, with units in °C, where (**c$_1$**) depicts the thermal structure evolution above the subducted slab, over 0 to 5 Myr, at the lower rate U_2.

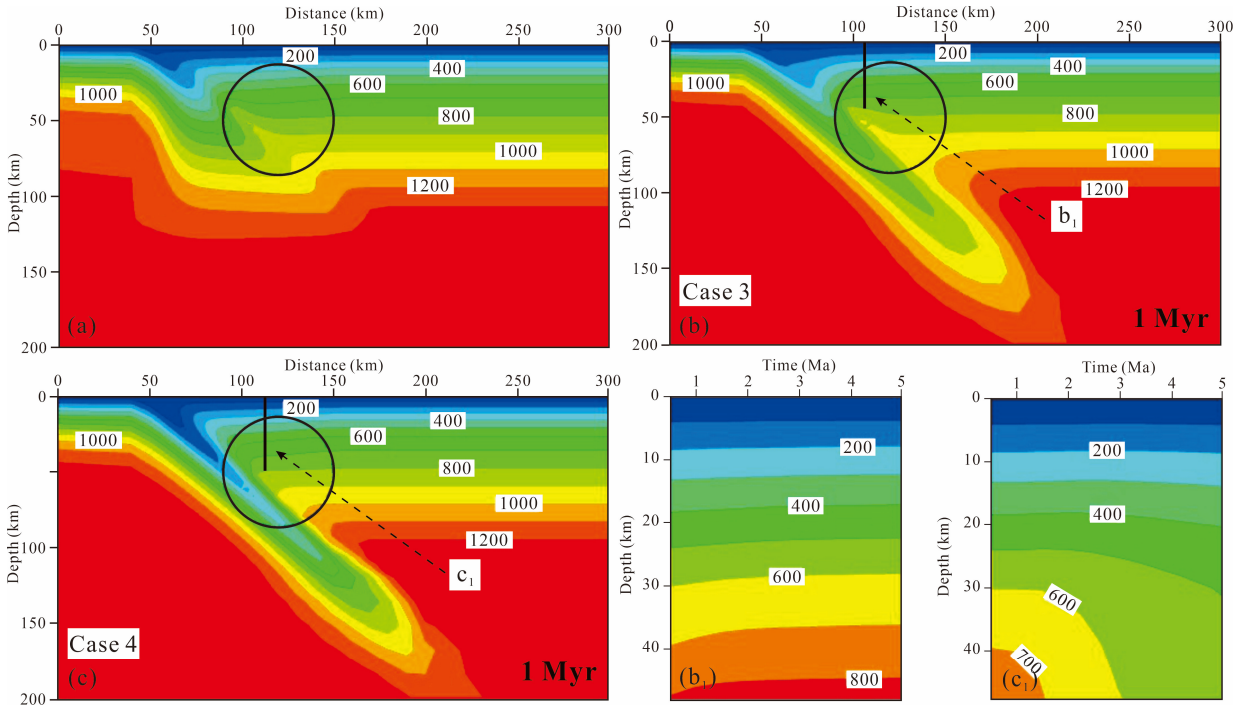


Figure 5. The effect of the subduction rate V on the evolution of thermal structure. (**a**) The current thermal structure, with units in °C; (**b**) Case 3: the thermal structure after 1 Myr at a lower subduction

rate V_1, also in °C, where (**b$_1$**) shows the evolution of the thermal structure above the subducted slab over 0 to 5 Myr at lower rate V_1; (**c**) Case 4: the thermal structure after 1 Myr at the higher subduction rate V_2, with units in °C, where (**c$_1$**) depicts the thermal structure evolution above the subducted slab over 0 to 5 Myr at the higher rate V_2.

4.2. Case 3 and Case 4: Same Overriding Plate Movement Rates, Different Subduction Rates

Figure 5 depicts the thermal structure of the subduction zone located beneath the Halmahera volcanic arc. This model was created with a constant overriding plate movement rate U_0 (around 5 cm/a), but with diverse subduction rates V. Specifically, Case 3 involves a subduction rate V_1 of approximately 2 cm/a, whereas Case 4 has a rate V_2 of about 4 cm/a.

The results reveal that following the subduction of the cold oceanic plate beneath the Halmahera volcanic arc, a low-temperature geosynclinal region developed beneath the overriding plate. In Case 3, a high-temperature anomaly zone emerged in the mantle wedge above the subduction interface, driven by friction and shear heating within the subduction zone. This led to a decrease in the depth at which rocks undergo brittle-ductile transformation. A vertical temperature gradient formed between the cooler subduction zone and the hotter mantle wedge above, and this inversion could remain stable for a prolonged duration (Figure 5b$_1$). Under these conditions, water released from the slab at depths greater than 100 km entered the mantle wedge, where temperatures were around 1000 °C. This condition was sufficient to induce partial melting and stimulate magmatism.

In Case 4, where the subduction rate was higher ($V_2 > V_1$), the friction and shear heating within the subduction zone decreased because the shallower rocks exhibited increased ductility. As a result, the vertical inversion of the high-temperature mantle wedge was dissipated along the subduction surface, leading to a reduced duration of the high-temperature anomaly (refer to Figure 5c$_1$). This had a limited effect on the magmatism of the volcanic arc. By analyzing Case 3 and Case 4, it can be inferred that when the movement rate of the overriding plate is consistent, a lower subduction rate facilitates the generation of higher temperatures in the mantle wedge. Additionally, the duration of the temperature anomaly in the mantle wedge is prolonged, which further supports the partial melting of mantle material and the subsequent formation of arc magmatic activity.

5. Discussion

When a subducting plate descends into the mantle, the components within a specific depth range under the volcanic arc can undergo partial melting to form magma, given the right conditions of temperature, pressure, and fluid. This magma then moves upwards, accumulates, and eventually erupts, creating arc volcanoes. The magmatic activity associated with subduction is predominantly influenced by factors such as temperature, pressure, and fluid presence (Figure 6a,b). To begin with, an increase in fluid content can significantly lower the melting point and solidus temperature of rocks. This factor also effects the melt's viscosity and the magma's average density [33,34]. Generally, volcanic arcs are believed to develop during subduction due to the dehydration of the descending slab, which leads to melting and magmatic eruptions after the mantle above the subducted slab becomes saturated with fluids [35]. Importantly, the depth at which the slab dehydrates plays a key role in influencing magmatic processes. If hornblende in the oceanic crust dehydrates shallowly, the partial melting of mantle rocks may be reduced even when the temperature of the mantle wedge exceeds 1000 °C at certain depths beneath the arc. This reduction occurs because a drier rock has a higher melting point, diminishing subduction-related magmatism [36]. Additionally, pressure affects rock melting, as it decreases the melting point. During the ascent of magma, decompression further melts the partial melt beneath the volcanic arc, which enhances the production of melting magma and speeds up its rise [37,38]. Lastly, elevated temperatures facilitate partial melting. In episodic fissure eruptions, the melting temperatures range between 700 and 900 °C for rhyolite and 1000 and 1300 °C for basalt. Thermal variations or disturbances during subduction can boost partial melting and modify magma composition.

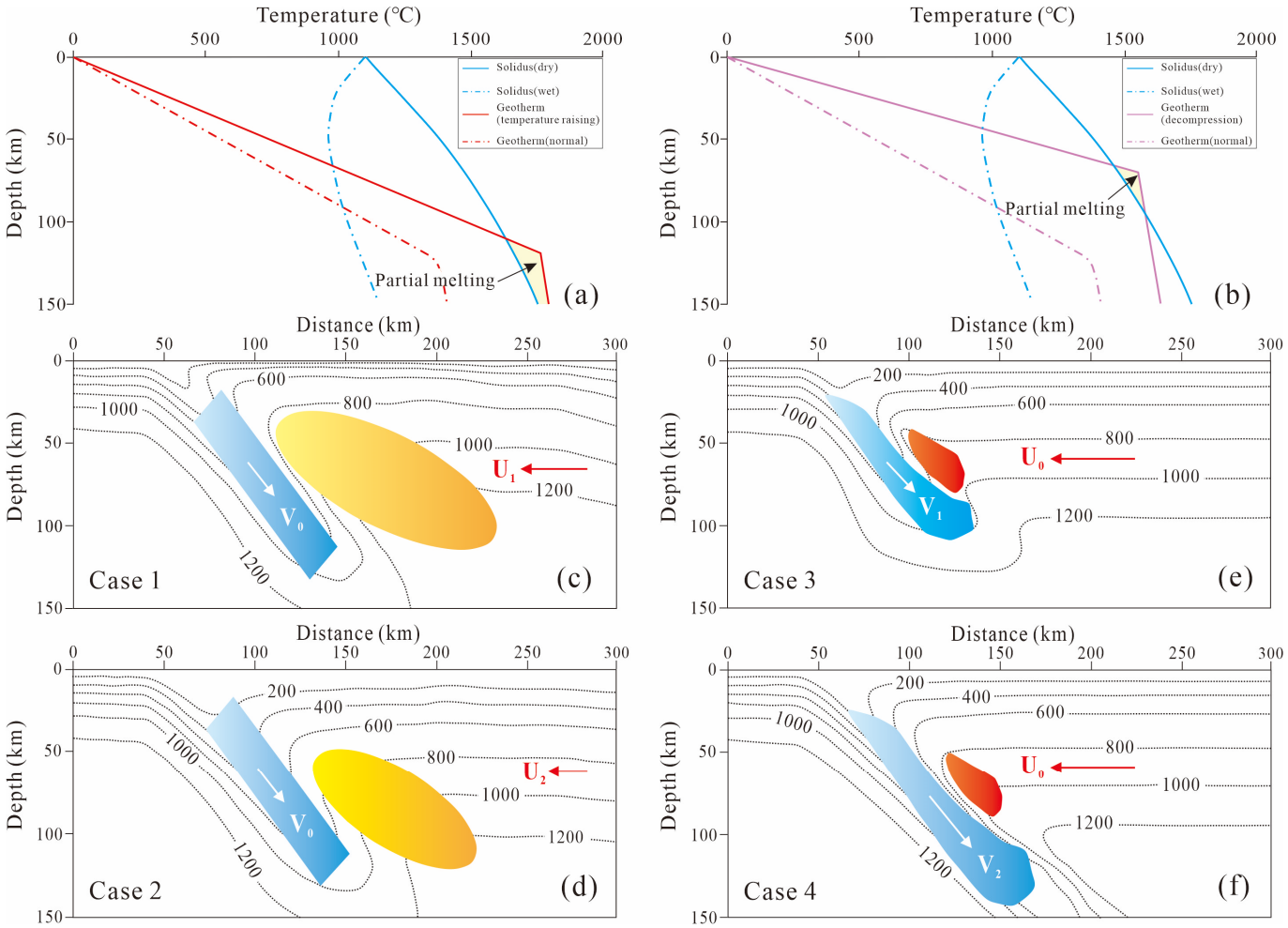


Figure 6. The analysis of volcanic arc magmatism is presented as follows: (**a**,**b**) illustrate factors affecting arc magmatism, including fluid effects, temperature effects, and pressure effects. (**c**,**d**) show the possible magmatism temperature ranges under constant subduction rates but varying overriding plate movement rates. (**e**,**f**) display the possible magmatism temperature ranges under constant overriding plate movement rates but varying subduction rates.

The depth at which the plate undergoes dehydration is influenced by the thermal structure of the subduction zone. When the depth of dehydration is optimal, the temperature profile of the mantle wedge controls arc magmatism. The thermal structure of the subduction zone is influenced by several factors, including subduction rates, the shape of the subducting slab, and shear friction heating [37]. In contrast, the temperature distribution within the mantle wedge is mainly governed by the overriding plate's movement rate, the properties of the lithosphere, and cooling rates. Thermal simulations have been employed to assess the temperature structures of the subduction zone and the mantle wedge beneath the Halmahera volcanic arc, accounting for different rates of subduction and movement of the overriding plate (Figure 6c–f).

As subduction progresses, the slab dehydrates at depths ranging from 100 km to 150 km, initiating partial melting of the mantle wedge material located above the subduction zone. This melting occurs at temperatures ranging from 800 to 1100 °C [35,39]. It follows that higher overriding plate movement rates (Case 1) or lower subduction rates (Case 3) are conducive to magma generation (Figure 6). The overriding plate movement rate is identified as the primary factor influencing the thermal structure of the mantle wedge. With a high movement rate of the overriding plate (Figure 6c), temperatures in the mantle wedge near the subduction zone rise significantly along the subduction slope, reaching

up to 900–1300 °C at 50–85 km above the subduction zone. Geochemical analyses of arc basalts show that partial melts with acidic components form at approximately 800 °C, while those with neutral components appear at around 1300 °C [40]. On the other hand, lower overriding plate movement rates (Figure 6d) cause mantle wedge temperatures near the subduction slope to be more influenced by the subduction process itself. This results in a reduction in the high-temperature zone above 800 °C, an increase in the depth at which partial melts form, and a decrease in the volume of melt, thereby diminishing its contribution to arc magmatism.

Figure 6e,f depict the temperature structures and magmatism depths for the same overriding plate movement rate U_0 but with different subduction rates ($V_1 < V_2$). At a lower subduction rate (Figure 6e), temperatures 50–85 km above the subduction zone range from 800 to 1000 °C, affected by shear friction heating. Hornblende minerals in the subducted oceanic crust dehydrate at depths below 100 km, where temperatures reach 900–1100 °C [35]. The water that is released subsequently migrates to the overriding shear heating zone, causing partial melting of the mantle wedge and promoting arc magmatism. [38,39]. Conversely, at a higher subduction rate (Figure 6f), the temperature in the mantle wedge decreases, which reduces the extent of dehydration at the same depth and its contribution to partial melting. Consequently, there is less mantle melting and diminished arc magmatism due to a reduced high-temperature zone from shear friction heating. Thus, it can be concluded that a higher overriding plate movement rate or a lower subduction rate facilitates the generation of higher temperatures in the mantle wedge. Furthermore, the duration of the high-temperature anomaly in the mantle wedge is extended, which further facilitates the partial melting of mantle material and the subsequent development of arc magmatic activity.

The plate tectonic reconstruction of the Halmahera arc and its periphery (Figure 7) reveals that the northward-drifting Australian plate collided with the southern part of the westward-drifting Halmahera arc approximately during the Early Miocene (20 Ma) to the Middle Miocene (15 Ma). Subsequently, from the Late Miocene (10 Ma) to the Early Pleistocene (2 Ma), the Australian plate persisted in drifting northward and rotating clockwise, and continued to push the southern part of the Halmahera arc (Obi Island) through the left-lateral strike-slip faults [41]. In the early Pleistocene (2 Ma), the Halmahera arc initiated a collision with the Sangihe forearc, leading to a deceleration in its westward migration [6,8]. The evolution of plate tectonics in Halmahera and its vicinity since 20 Ma (Figure 7b) illustrates that the southern part of the Halmahera arc (Obi Island) has been accelerated due to the persistent northwestward pushing of the Australian plate since the Middle Miocene, increasing the movement rate of the overriding microplate in the south. Videlicet, the movement rate of Obi Island microplate in the south is greater than that of the "K shape" Halmahera Island microplate in the north, corresponding to Case 1 and Case 2, as depicted in the simulation results above.

Thus, the dynamic cause of volcanic age disparity between the northern and southern parts of the Halmahera arc can be concluded. Since the Early Miocene (20 Ma), the Australian plate has persistently drifted northward. Around the Middle Miocene (15 Ma), the Halmahera subduction initiated, and the Halmahera subduction zone retreated westward with the subduction. At this juncture, the Australian plate kept drifting northward and continuously pushed the Obi Island microplate in the southern part of the Halmahera arc via the left-lateral strike-slip faults (Figure 8a). Owing to the pushing of the Australian plate, the movement rate of the Obi Island microplate in the south was increased (U_1 is approximately 6 cm/a) (Figure 8c), while that of Halmahera Island microplate in the north was relatively low (U_2 is approximately 4 cm/a) as it was hardly affected by the pushing of the Australian plate (Figure 8b). As depicted in Figure 8c, the Obi Island microplate in the south moved at a higher rate and formed a high-temperature area favorable for arc magmatic activity faster above the slope of the subduction zone, thereby leading to the earlier formation of the Obi Island arc volcanic activity in the late Miocene (10 Ma). In contrast, Halmahera Island microplate in the north moved at a relatively lower rate,

and it took a longer time to form a high-temperature zone conducive to magmatic activity beneath the arc, resulting in the later formation of the Halmahera arc volcanic activity in the late Pliocene (5 Ma) (Figure 8b).

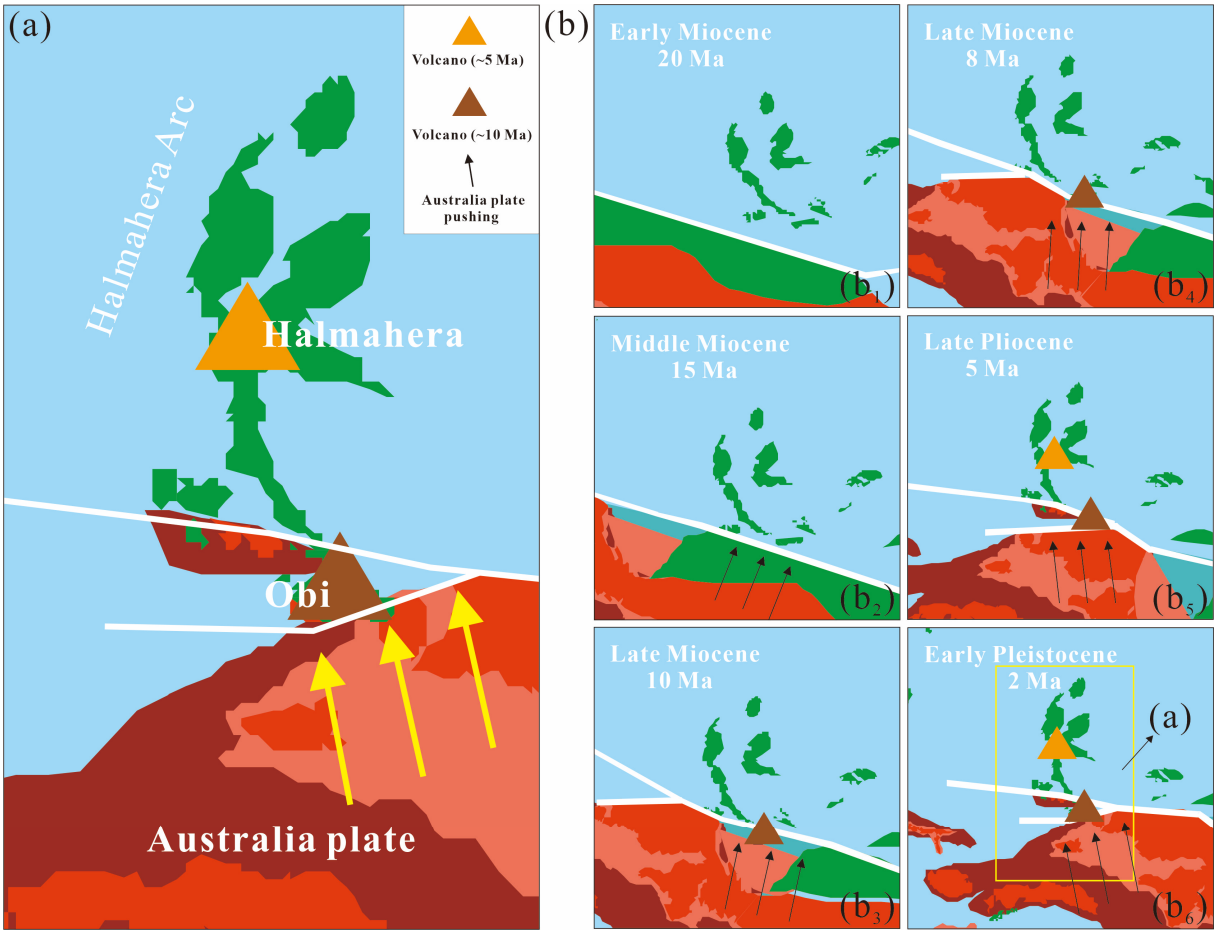


Figure 7. Plate tectonic reconstruction in the Halmahera arc and its vicinity (modified after [6,8]). (**a**) The plate tectonics in the Halmahera arc and its vicinity at 2 Ma, where the yellow arrow represents the pushing of the Australian plate against the Halmahera arc. (**b**) The evolution of plate tectonics in Halmahera and its vicinity since 20 Ma. The black arrow represents the pushing of the Australian plate against the Halmahera arc. (**b1**–**b6**) are the plate tectonic characteristics of each stage.

It is significant to note that the arc magmatism induced by subduction is primarily governed by temperature, pressure, and fluid. Our thermal simulation primarily examines how plate movement rate affects mantle wedge temperature as the subducting plate reaches dehydration depth. However, it does not consider the pressure factor. Pressure is indeed important in affecting rock melting, as the melting point of rocks decreases with increasing pressure. During upward migration, the partial melt beneath the volcanic arc experiences pressure reduction, which can further induce melting, thereby enhancing the supply of molten magma and accelerating its ascent [37]. Nevertheless, this process is highly complex and is typically affected by many factors, such as the upward migration distance and the thickness of the overriding lithosphere, which fall outside the scope of our research. Consequently, our results represent only one potential dynamic explanation for the volcanic age disparity observed in the Halmahera arc. The underlying causes for these differences are likely to be more intricate and varied, necessitating additional data and more comprehensive models for further investigation.

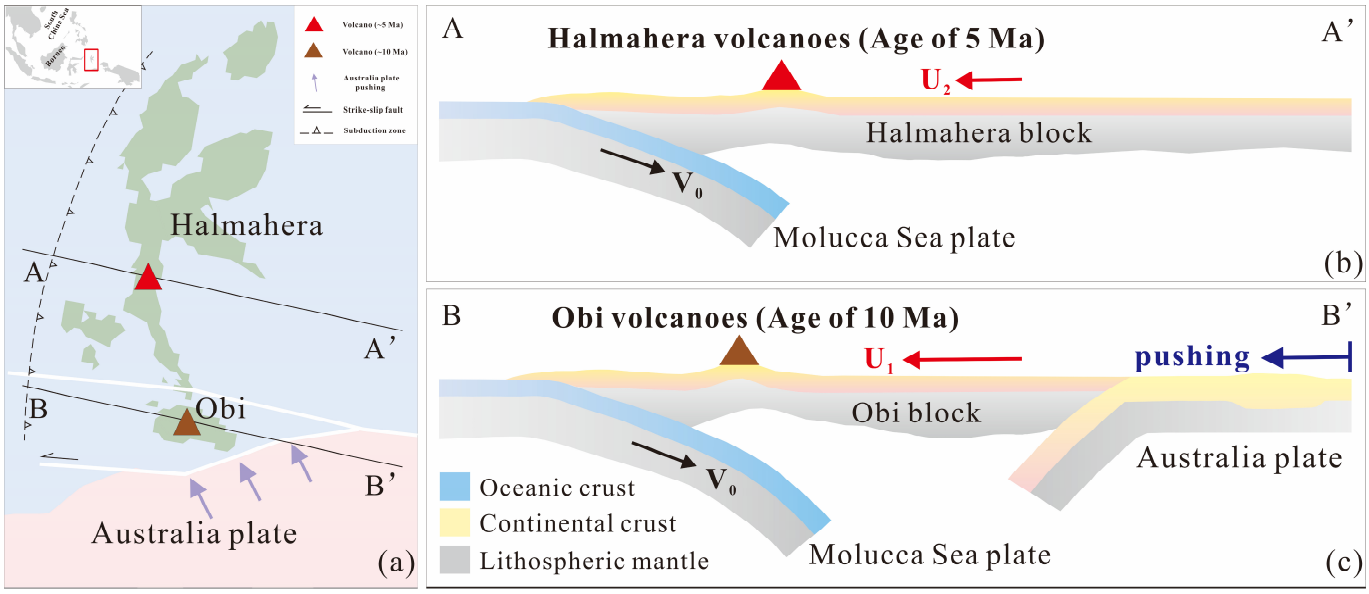


Figure 8. The explanation of the cause of volcanic age differences in Halmahera arc. (**a**) Tectonic setting of the Halmahera arc and its vicinity. (**b**) The cause of the young volcanic age in Halmahera Island in the north. (**c**) The cause of the old volcanic age in Obi Island in the south.

6. Conclusions

Based on the thermal simulations and dynamic analysis of the Halmahera arc and its periphery presented in this paper, the following conclusions are drawn. The thermal simulation results reveal that the depth of oceanic crust dehydration in the subduction zone and the mantle wedge temperature structure are strongly affected by both the plate subduction rate and the overriding plate movement rate. When the subduction rate is constant, a higher overriding plate movement rate promotes arc magmatism. Conversely, for a fixed overriding plate movement rate, a lower subduction rate enhances the potential for arc magmatism. The disparity in volcanic age within the Halmahera arc is attributed to the varying movement rates of the overriding microplates in the subduction zone. During the Middle Miocene, the Australian plate drifted northward and persistently pushed the Obi Island microplate in the south via the left-lateral strike-slip faults, augmenting its movement rate. In contrast, the movement rate of Halmahera Island microplate in the north was slow, as it was hardly affected by the Australian plate. The Obi Island microplate in the south moved at a higher rate and formed a high-temperature area conducive to arc magmatic activity more rapidly above the slope of the subduction zone, thereby facilitating the earlier formation of the Obi Island arc's volcanic activity in the late Miocene (10 Ma). Conversely, the Halmahera Island microplate in the north moved at a relatively lower rate, and it took a longer time to form a high-temperature zone favorable for magmatic activity beneath the arc, giving rise to the later formation of the Halmahera arc volcanic activity in the late Pliocene (5 Ma). Our results enhance the understanding of magmatism and dynamics in the Halmahera arc and its surroundings. Additionally, they offer a valuable thermal simulation method for future studies of similar retreating subduction zone island arc volcanoes.

Author Contributions: Conceptualization, formal analysis, methodology, software, writing—original draft, G.F. (Gui Fang); conceptualization, writing—review and editing, X.W.; supervision, G.F. (Guozhang Fan); validation, H.W.; methodology, G.Z.; investigation, Z.Y.; supervision, J.Z. All authors have read and agreed to the published version of the manuscript.

Funding: This research was funded by the Petrochina Basic and Frontier Science and Technology Project (No. 2024ZZ5601), the National Natural Science Foundation of China (Grant Nos. 42176052, 42276072).

Institutional Review Board Statement: Not applicable.

Informed Consent Statement: Not applicable.

Data Availability Statement: The raw data supporting the conclusions of this article will be made available by the authors on request.

Acknowledgments: The research was conducted at the National Supercomputer Center located in Tianjin, utilizing the Tianhe new-generation supercomputer for calculations. Most of the figures presented in this paper were created using Generic Mapping Tools (GMT). We express our gratitude to the Computational Infrastructure for Geodynamics (geodynamics.org, accessed on 3 August 2024) for facilitating the development of ASPECT. The open-source software ASPECT is available for download at the website (https://geodynamics.org/, accessed on 10 August 2024).

Conflicts of Interest: The authors declare no conflicts of interest.

References

1. Hamilton, W.H. *Tectonics of the Indonesian Region*; U.S. Geology Survey Professional Paper 1078; United States Government Printing Office: Washington, DC, USA, 1979; p. 345p. [CrossRef]
2. Mccaffrey, R.; Silver, E.A.; Raitt, R.W. Crustal structure of the Molucca Sea collision zone, Indonesia. In *The Tectonic and Geologic Evolution of Southeast Asian Seas and Islands*; AGU: Washington, DC, USA, 1980; pp. 161–177. [CrossRef]
3. Puspito, N.T.; Yamanaka, Y.; Miyatake, T.; Shimazaki, K.; Hirahara, K. Three-dimensional P-wave velocity structure beneath the Indonesian region. *Tectonophysics* **1993**, *220*, 175–192. [CrossRef]
4. Hall, R.; Ali, J.R.; Anderson, C.D. Cenozoic motion of the Philippine Sea plate: Palaeomagnetic evidence from eastern Indonesia. *Tectonics* **1995**, *14*, 1117–1132. [CrossRef]
5. Rangin, C.; Le Pichon, X.; Mazzotti, S.; Pubellier, M.; Chamot-Rooke, N.; Aurelio, M.; Walpersdorf, A.; Quebral, R. Plate convergence measured by GPS across the Sundaland/Philippine Sea plate deformed boundary: The Philippines and eastern Indonesia. *Geophys. J. Int.* **1999**, *139*, 296–316. [CrossRef]
6. Hall, R. Late Jurassic–Cenozoic reconstructions of the Indonesian region and the Indian Ocean. *Tectonophysics* **2012**, *570–571*, 1–41. [CrossRef]
7. Hamilton, W.B. Plate tectonics and island arcs. *Geol. Soc. Am. Bull.* **1988**, *100*, 1503–1527. [CrossRef]
8. Hall, R.; Smyth, H.R. Cenozoic arc processes in Indonesia: Identification of the key influences on the stratigraphic record in active volcanic arcs. *Geol. Soc. Am.* **2008**, *436*, 27–45. [CrossRef]
9. Hall, R. Cenozoic geological and plate tectonic evolution of SE Asia and the SW Pacific: Computer-based reconstructions, model and animations. *J. Asian Earth Sci.* **2002**, *20*, 353–431. [CrossRef]
10. Hall, R.; Spakman, W. Subducted slabs beneath the eastern Indonesia–Tonga region: Insights from tomography. *Earth Planet. Sci. Lett.* **2002**, *201*, 321–336. [CrossRef]
11. Baker, S.; Malaihollo, J. Dating of Neogene igneous rocks in the Halmahera region: Arc initiation and development. *Geol. Soc. Lond. Spec. Publ.* **1996**, *106*, 499–509. [CrossRef]
12. Cardwell, R.; Isaacks, B.; Karig, D. The spatial distribution of earthquakes, focal mechanism solutions, and subducted lithosphere in the Philippine and northeastern Indonesian islands. In *The Tectonic and Geologic Evolution of Southeast Asian Seas and Islands*; Geophysical Monograph Series; AGU: Washington, DC, USA, 1980; Volume 23, pp. 1–35. [CrossRef]
13. Hall, R. Plate boundary evolution in the Halmahera region, Indonesia. *Tectonophysics* **1987**, *144*, 337–352. [CrossRef]
14. Hall, R. The subduction initiation stage of the Wilson cycle. *Geol. Soc. Lond. Spec. Publ.* **2019**, *470*, 415–437. [CrossRef]
15. Dong, M.; Zhang, J.; Jiang, C.; Hao, T.; Xu, Y.; Huang, S.; Liu, L.; Nan, F.; Fang, G. Thermal simulation of migration mechanism of the Halmahera volcanic arc, Indonesia. *J. Asian Earth Sci.* **2021**, *232*, 105042. [CrossRef]
16. Stern, R.J.; Gerya, T. Subduction initiation in nature and models: A review. *Tectonophysics* **2018**, *746*, 173–198. [CrossRef]
17. Hinschberger, F.; Malod, J.-A.; Réhault, J.-P.; Villeneuve, M.; Royer, J.-Y.; Burhanuddin, S. Late Cenozoic geodynamic evolution of eastern Indonesia. *Tectonophysics* **2005**, *404*, 91–118. [CrossRef]
18. Gaina, C.; Müller, D. Cenozoic tectonic and depth/age evolution of the Indonesian gateway and associated back-arc basins. *Earth-Sci. Rev.* **2007**, *83*, 177–203. [CrossRef]
19. Konopka, G.; Szamałek, K.; Zglinicki, K. Ni-Co bearing laterites from Halmahera Island (Indonesia). *Appl. Sci.* **2022**, *12*, 7586. [CrossRef]
20. Hall, R.; Audley-Charle, M.; Banner, F.; Hidayat, S.; Tobing, S. Basement rocks of the Halmahera region, eastern Indonesia: A Late Cretaceous–early Tertiary arc and fore-arc. *J. Geol. Soc.* **1988**, *145*, 65–84. [CrossRef]
21. Waltham, D.; Hall, R.; Smyth, H.R.; Ebinger, C.J. Basin formation by volcanic arc loading. *Spec. Pap. Geol. Soc. Am.* **2008**, *436*, 11–26. [CrossRef]
22. International Seismological Centre. On-Line Bulletin. 2024. Available online: www.isc.ac.uk (accessed on 5 August 2024).
23. Global Wave Velocity Anomaly Model UU-P07. Online Bulletin. 2024. Available online: http://www.atlas-of-the-underworld.org (accessed on 5 August 2024).

24. Global Gravity Database TOPEX. Online Bulletin. 2024. Available online: https://topex.ucsd.edu/marine_topo/ (accessed on 6 August 2024).
25. Liu, C.; Shi, Y.L. The role of fault interaction on earthquake migration in central Sulawesi. Indonesia. *Tectonophysics* **2022**, *839*, 229530. [CrossRef]
26. Zhang, J.; Hao, T.; Dong, M.; Xu, Y.; Wang, B.; Ai, Y.; Fang, G. Investigation of geothermal structure of the Sulawesi, using gravity and magnetic method. *Sci. China Earth Sci.* **2020**, *64*, 278–293. [CrossRef]
27. Milsom, J. Subduction in eastern Indonesia: How many slabs. *Tectonophysics* **2001**, *338*, 167–178. [CrossRef]
28. Kronbichler, M.; Heister, T.; Bangerth, W. High accuracy mantle convection simulation through modern numerical methods. *Geophys. J. Int.* **2012**, *191*, 12–29. [CrossRef]
29. Zhang, Q.; Guo, F.; Zhao, L.; Wu, Y. Geodynamics of divergent double subduction: 3-D numerical modeling of a Cenozoic example in the Molucca Sea region, Indonesia. *J. Geophys. Res. Solid Earth* **2017**, *122*, 3977–3998. [CrossRef]
30. Song, T.; Hao, T.; Zhang, J.; Cao, L.; Dong, M. Numerical modeling of North Sulawesi subduction zone: Implications for the east–west differential evolution. *Tectonophysics* **2022**, *822*, 229172. [CrossRef]
31. Fang, G.; Zhang, J.; Hao, T.; Dong, M.; Jiang, C.; He, Y. The causal mechanism of the Sangihe Forearc Thrust, Molucca Sea, northeast Indonesia, from numerical simulation. *J. Asian Earth Sci.* **2022**, *237*, 105350. [CrossRef]
32. Yu, L.; Zhang, J.; Dong, M.; Fang, G.; Yu, L. Magmatism-Related Thermal Simulation of Volcanic Arcs in the Molucca Sea Bidirectional Subduction System. *J. Ocean Univ. China* **2023**, *22*, 939–948. [CrossRef]
33. Turcotte, D.L.; Schubert, G. *Geodynamics*; Cambridge University Press: Cambridge, UK, 2014.
34. Pearce, J.A.; Peate, D.W. Tectonic implications of the composition of volcanic ARC magmas. *Annu. Rev. Earth Planet. Sci.* **1995**, *23*, 251–285. [CrossRef]
35. William, J.C.; Murphy, J.B.; Johnson, T.E.; Huiqing, H. Critical role of water in the formation of continental crust. *Nat. Geosci.* **2020**, *13*, 331–338. [CrossRef]
36. Chen, L.; Faccenda, M. Subduction-induced upwelling of a hydrous transition zone: Implications for the Cenozoic magmatism in northeast China. *J. Geophys. Res. Solid Earth* **2019**, *124*, 11489–11504. [CrossRef]
37. Hall, P.S.; Kincaid, C. Diapiric Flow at Subduction Zones: A Recipe for Rapid Transport. *Science* **2001**, *292*, 2472–2475. [CrossRef]
38. Peacock, S.M.; Rudhmer, T.; Thompson, A.B. Pareial melting of subducting oceanic crust. *Earth Planet. Sci. Lett.* **1994**, *121*, 227–244. [CrossRef]
39. Widiyantoro, S.; van der Hilst, R. Mantle structure beneath Indonesia inferred from high-resolution tomographic imaging. *Geophys. J. Int.* **1997**, *130*, 167–182. [CrossRef]
40. Thybo, H.; Artemieva, I.M. Moho and magmatic underplating in continental lithosphere. *Tectonophysics* **2013**, *609*, 605–619. [CrossRef]
41. Aprina, P.U.; Santoso, D.; Alawiyah, S.; Prasetyo, N.; Ibrahim, K. Delineating geological structure utilizing integration of remote sensing and gravity data: A study from Halmahera, North Molucca, Indonesia. *Vietnam J. Earth Sci.* **2024**, *46*, 147–167. [CrossRef]

Disclaimer/Publisher's Note: The statements, opinions and data contained in all publications are solely those of the individual author(s) and contributor(s) and not of MDPI and/or the editor(s). MDPI and/or the editor(s) disclaim responsibility for any injury to people or property resulting from any ideas, methods, instructions or products referred to in the content.